TYPE Original Research
PUBLISHED 06 November 2025
DOI 10.3389/feart.2025.1678611



#### **OPEN ACCESS**

EDITED BY Baehyun Min, Ewha Womans University, Republic of Korea

Zhengzheng Cao, Henan Polytechnic University, China Buraq Adnan Al-Baldawi, University of Baghdad, Iraq

\*CORRESPONDENCE
Liming Zhang,

☑ zhangliming@upc.edu.cn

RECEIVED 05 August 2025 REVISED 02 October 2025 ACCEPTED 14 October 2025 PUBLISHED 06 November 2025

#### CITATION

Ji Y and Zhang L (2025) A method for analyzing interwell connectivity based on gated recurrent network with knowledge interaction.

Front. Earth Sci. 13:1678611. doi: 10.3389/feart.2025.1678611

#### COPYRIGHT

© 2025 Ji and Zhang. This is an open-access article distributed under the terms of the Creative Commons Attribution License (CC BY). The use, distribution or reproduction in other forums is permitted, provided the original author(s) and the copyright owner(s) are credited and that the original publication in this journal is cited, in accordance with accepted academic practice. No use, distribution or reproduction is permitted which does not comply with these terms.

# A method for analyzing interwell connectivity based on gated recurrent network with knowledge interaction

Yingchun Ji<sup>1</sup> and Liming Zhang<sup>2</sup>\*

<sup>1</sup>Exploration and Development Research Institute of Sinopec Shengli Oil Field Company, Dongying, Shandong, China, <sup>2</sup>School of Petroleum Engineering, China University of Petroleum (East China), Qingdao, China

Traditional interwell connectivity analysis methods for water-flooding reservoirs suffer from two major limitations: insufficient integration of seepage physics, leading to poor interpretability, and inadequate temporal modeling, which fails to capture the dynamic evolution of injection-production relationships. To overcome these issues, this study proposes a Knowledge-Interactive Gated Recurrent Unit (KIGRU) model that integrates physical constraints with temporal deep learning. The model adopts a dual-subnet architecture: Net-INJ encodes injection rates and interwell connectivity through gate functions and connection matrices, while Net-VOL characterizes reservoir volume changes. By embedding material balance equations into the network design, the model ensures physical consistency, while GRU modules effectively capture long-term temporal dependencies. Numerical experiments on synthetic reservoir cases demonstrate that KIGRU outperforms conventional neural networks and the Capacitance-Resistance Model (CRM) in both history matching and production forecasting. The model accurately identifies high-permeability channels, quantifies nonequilibrium flow, and yields more reliable predictions of liquid production rates. These results confirm that KIGRU achieves a balance between physical interpretability and predictive accuracy, offering a practical and theoretically sound tool for interwell connectivity analysis.

KEYWORDS

machine learning, water-flooding reservoir, gated recurrent unit, well connectivity analysis, neural network

#### 1 Introduction

Water-flooding is the primary enhanced oil recovery method in China's oil and gas fields, where addressing injection-production contradictions is critical for maximizing recovery efficiency (Hernandez-Mejia et al., 2023). During reservoir development, high-permeability channels cause premature water breakthrough at production wells (Zhang H. et al., 2022; Dai et al., 2025; Gu et al., 2021), preventing injected fluids from reaching low-permeability zones and effectively displacing remaining oil. This creates an inefficient cycle of high water injection and high water production, leading to significant resource waste and limited recovery improvement (Wang et al., 2023; Karpatne et al., 2017). Inter-well connectivity analysis determines the flow communication patterns between injection and production wells, providing essential

guidance for hydrodynamic adjustments, chemical plugging operations, and injection-production optimization strategies (Yousef et al., 2009; Yousef et al., 2006). Therefore, accurate connectivity characterization represents a key component of reservoir development dynamics analysis, with direct practical value for comprehensive field management, remaining oil distribution mapping, and water-flooding performance enhancement.

Recent advances in artificial intelligence have accelerated the intelligentization of petroleum engineering (Haghighat et al., 2021; Meng and Karniadakis, 2020; Abbasi and Andersen, 2024), offering new approaches to address the growing challenges of global energy demand. Oil and gas companies increasingly utilize new information technology and intelligent management processes to improve efficiency and enhance development outcomes (Nagao et al., 2024; Zhang K. et al., 2022). Data-driven models based on injectionproduction dynamics can learn correlation relationships to predict well performance and evaluate field capacity (Chung et al., 2014; Xu et al., 2022; Chen et al., 2021). Among these, artificial neural networks can construct nonlinear mappings between injection rates and production rates, with network weights inversely representing inter-well connectivity. To enhance the reliability and applicability of neural network-based connectivity analysis, recent research has evolved along two complementary directions: physics-informed approaches that embed physical constraints and governing equations into model architectures, and temporal modeling architectures that leverage recurrent neural networks to capture dynamic injection-production relationships over time (Li et al., 2024; Yu et al., 2023; Huang et al., 2024; Zeng et al., 2022).

To overcome the limitations of traditional artificial neural networks, recent research has focused on developing more sophisticated deep learning architectures that incorporate physical constraints and interpretable mechanisms. Physics-informed neural networks (PINNs) have gained significant attention in reservoir engineering applications, demonstrating the capability to embed governing equations and physical constraints directly into the neural network training process (Raissi et al., 2019; Fraces and Hamdi, 2021; Wen et al., 2021). Recent studies have successfully applied PINNs to reservoir pressure prediction, history matching, and production optimization, showing improved generalization compared to purely data-driven approaches (Tang et al., 2020; Wang N. et al., 2021; Mudunuru, 2020). However, PINNs face critical limitations when applied to dynamic interwell connectivity analysis: their formulation typically assumes static or quasistatic physical relationships, making it challenging to model the time-evolving nature of injection-production responses where historical patterns create cumulative effects on current reservoir behavior (Almajid and Abu-Al-Saud, 2022; Harp et al., 2021). Furthermore, while PINNs excel at enforcing known physical laws, they struggle to simultaneously capture complex temporal dependencies and spatial heterogeneity in multi-well systems with long-term historical data (Alakee et al., 2020).

In modeling temporal dynamics of oilfield production data, researchers have explored various time-series approaches for injection-production relationships. Traditional methods often assume static or quasi-static connectivity patterns, failing to capture the dynamic evolution of reservoir flow behavior over time. Gated recurrent units (GRUs) and long short-term memory (LSTM) networks have demonstrated strong capabilities in

modeling sequential production data, effectively capturing temporal dependencies and long-term correlations in injection-production dynamics (Yu et al., 2023; Jiang et al., 2022). These recurrent architectures process time-series information through internal memory mechanisms, enabling them to learn how injection rate variations propagate through the reservoir and influence production responses at different time lags (Al-Shabandar et al., 2020). Recent advances in attention mechanisms and transformer architectures have further enhanced temporal modeling by explicitly quantifying time-varying influence relationships between injection and production wells, allowing the model to adaptively weight historical information based on temporal relevance (Wang H. et al., 2021). Despite these developments in temporal modeling techniques, significant challenges remain in simultaneously achieving accurate time-series prediction while maintaining physically meaningful representations of reservoir connectivity for water-flooding analysis.

However, despite these methodological advances, practical application reveals significant limitations in both physicsinformed and temporal modeling approaches. Physics-informed neural networks, while capable of embedding physical laws into the learning process through loss function constraints, are fundamentally designed for static or quasi-static problems and cannot effectively model the dynamic temporal evolution of injection-production responses, where historical patterns create time-dependent cumulative effects on reservoir behavior. Conversely, RNN-based architectures, though effective at capturing temporal sequences and long-term dependencies, operate as blackbox models that lack mechanisms to incorporate fundamental seepage physics, limiting their ability to produce physically meaningful connectivity parameters that satisfy Darcy flow principles. For instance, when analyzing long-term waterflood performance in mature fields, PINN approaches struggle to capture the delayed response characteristics because their framework assumes instantaneous physical equilibrium, while conventional RNN models evaluate injection-production relationships based purely on data patterns without ensuring compliance with porous media flow mechanics. These modeling challenges are further compounded by the complex physical processes occurring within reservoir systems. Recent experimental advances in nuclear magnetic resonance (NMR) techniques have provided new insights into pore structure evolution and permeability changes under stress conditions (Wang and Chen, 2023), while studies on thermo-mechanical degradation in low-permeability formations have revealed how temperature cycling affects fracture networks and connectivity pathways (Teng et al., 2025). These findings underscore the complexity of reservoir connectivity dynamics and highlight the need for modeling approaches that can simultaneously capture temporal evolution while respecting fundamental physical constraints governing fluid flow in porous media.

To address these critical research gaps and overcome the fundamental limitations of existing approaches, there is an urgent need for a method that combines two essential capabilities: (1) physics-informed architecture to ensure model parameters have clear physical interpretations. (2) temporal modeling to capture the dynamic evolution of injection-production relationships. This paper proposes a novel inter-well connectivity analysis method for water-flooding reservoirs based on a knowledge-interacting gated recurrent network model to address the aforementioned

issues. Firstly, the material balance equation for injection and production is integrated into the construction process of the machine learning model, endowing the model parameters with clear physical meanings related to percolation, effectively enhancing the interpretability of the machine learning model in connectivity analysis. Additionally, the model employs a gated recurrent unit structure to consider the impact of historical water injection on the current production moment, thereby improving the model's prediction accuracy for liquid production rate and water-cut. This method overcomes the limitations of both traditional physical methods and general machine learning approaches (Wang et al., 2025). It provides a new solution for connectivity analysis of water-flooding reservoirs with significant theoretical and practical value.

# 2 Inter-well connectivity analysis in water-flooding reservoirs

# 2.1 Material balance equation for water-flooding reservoirs

The material balance equation is one of the fundamental percolation principles for multi-phase flow in fluid-porous media systems. Assuming a single-source and single-sink water-flooding reservoir development scenario with only oil-water two-phase flow, and disregarding the effects of capillary forces, gravity, and reservoir boundary conditions, the material balance equation can be described as follows (Equation 1):

$$C_t V_p \frac{\mathrm{d}\overline{p}}{\mathrm{d}t} = i(t) - q(t) \tag{1}$$

where  $C_t$  represents the comprehensive compression coefficient, MPa<sup>-1</sup>;  $V_p$  is the control volume of the production well, m<sup>3</sup>;  $\overline{p}$  represents the average formation pressure, MPa; i(t) and q(t) and respectively represent the water injection and production rates of the water injection well and production well at time step t, m<sup>3</sup>·d<sup>-1</sup>.

Based on this, extending to the development scenario of M injection wells and N production wells, the injection-production material balance equation centered on the nth production well can be described as Equation 2:

$$\sum_{m=1}^{M} C_t^{mn} V_p^{mn} \frac{\mathrm{d}\overline{p}^{mn}}{\mathrm{d}t} = \sum_{m=1}^{M} \beta^{mn} i^m(t) - q_j(t)$$
 (2)

where  $m \in [1,2,...,M]$  and  $n \in [1,2,...,N]$  represent the indices of injection wells and production wells, respectively;  $\beta^{mn}$  is the connectivity coefficient between the mth injection well and the nth production well, and  $i^m(t)$  is the injection rate of the mth injection well at time t.

## 2.2 Inter-well connectivity representation of water-flooding reservoirs

For the development scenarios of M water injection wells and N production wells, considering the closed reservoir boundary conditions, the connectivity coefficient corresponding to the mth water injection well should satisfy the constraint that the sum of the

splitting coefficients for each production well it flows to should be 1, that is Equation 3:

$$\left| \sum_{n=1}^{N} \beta^{mn} - 1 \right| = 0 \tag{3}$$

Taking into account the situation of M wells, the connectivity coefficients in the entire block should satisfy the following constraints (Equation 4):

$$\sum_{m=1}^{M} \left( \left| \sum_{n=1}^{N} \beta^{mn} - 1 \right| \right) = 0 \tag{4}$$

To ensure the connectivity coefficients satisfy the unit sum constraint during training, a softmax normalization layer is applied to the raw connectivity outputs (Equation 5):

$$\beta_{mn} = \frac{exp(\hat{\beta}_{mn})}{\sum_{k=1}^{N} exp(\hat{\beta}_{mn})}$$
 (5)

where  $\beta_{mn}$  represents the raw (unconstrained) connectivity coefficient output from the KIGRU network for injection well m to production well n.

At each training iteration, the constraints are automatically verified (Equation 6):

$$abs\left(\sum_{m=1}^{N}\beta_{mn}-1\right) < \epsilon, \qquad \forall m \tag{6}$$

where  $\epsilon$  is a small tolerance value (typically  $10^{-6}$ ).

# 3 Knowledge interactive gated recurrent network modeling

#### 3.1 Recursive neural network

The Recurrent Neural Network (RNN) (Nagao et al., 2024) is a deep learning model suitable for processing data with sequential structures. A key feature of RNN is its "recurrent" structure, which allows the model state at each time step to be composed of the input at the current time step and the state (known as the hidden state) passed from the previous time step, used for output calculation at the current time step and state calculation for the next time step. The forward propagation calculation process is as follows (Equations 7, 8):

$$h_{t} = f(U_{h}x_{t} + V_{h}h_{t-1} + b_{h})$$
(7)

$$y_t = g(Wh_t + b_y) \tag{8}$$

where  $x_t$  represents the model input at time t,  $h_{t-1}$  denotes the hidden state at time t-1,  $h_t$  signifies the hidden state at time t,  $U_h$ ,  $V_h$ , and W are network weights,  $b_h$  and  $b_y$  are network biases, f and g are activation functions, and  $y_t$  stands for the model output at time t.

During the back-propagation process of RNN, the gradient (i.e., error signal) may gradually become very small when propagating between multiple layers, resulting in the phenomenon of gradient vanishing and leading to stagnation in the learning process. This issue is particularly prominent when dealing with long

sequences. Because long sequences increase the number of steps for gradient propagation between multiple layers, thereby increasing the risk of gradient vanishing. The root cause of this problem lies in the design structure of RNN. To overcome this limitation, many researchers have proposed variants such as LSTM (Long Short-Term Memory) (Zhang K. et al., 2022) and GRU (Gated Recurrent Unit) (Chung et al., 2014) models. Compared to LSTM, GRU has fewer parameters, lower computational cost, faster convergence speed, and higher learning efficiency. Therefore, the model used in this paper is developed based on GRU.

As illustrated in the model architecture, two parallel GRUbased subnets (Net-INJ and Net-VOL) are employed to capture the temporal dynamics of different physical processes in the reservoir system. Net-INJ processes injection rate descriptions combined with gate functions through a connection matrix, while Net-VOL handles volume change descriptions incorporating both injection rate and pressure data. Each subnet utilizes GRU cells with hidden states (h<sub>1</sub> and h<sub>2</sub>) that can effectively preserve long-term dependencies through their reset and update gate mechanisms. The temporal knowledge extraction networks within both subnets enable the model to learn complex sequential patterns from historical data, with the reset gates controlling information retention and update gates determining the integration of new inputs. This dual-subnet architecture allows the model to simultaneously learn injection-related dynamics and volume changes, ultimately generating predictions for liquid production rate through their combined outputs, thereby addressing the multi-physics coupling challenges inherent in reservoir production forecasting.

## 3.2 Knowledge interactive gated recurrent network model

The distribution of oil-water two-phase flow is influenced not only by fluid properties (such as viscosity), but also by the physical heterogeneity of the reservoir rock (such as porosity, permeability, etc.) (Xu et al., 2022; Chen et al., 2021). Therefore, the underground flow pattern exhibits strong uncertainty. The complex nonlinear relationship between injection and production signals is primarily manifested on the time scale of reservoir development. Reservoir numerical simulators can accurately simulate the injectionproduction relationship, but modeling requires geological attribute parameters such as permeability, porosity, and saturation for each grid, and obtaining these geological attributes through well logging is very costly. Additionally, as the size of the reservoir increases, the computational cost of numerical simulators also increases, and completing a simulation for a large-scale reservoir can take tens of minutes or even hours (Huang et al., 2024; Zeng et al., 2022). Under the framework of machine learning integrated with the material balance equation for water-flooding reservoirs, this paper proposes a Knowledge Interaction Gated Recurrent Unit (KIGRU) model. Guided by the material balance equation for water-flooding reservoirs, the KIGRU model considers the impact of reservoir boundary conditions on the injection-production relationship. By coupling injection-production dynamic information on a time scale, it uses a modular parallel computing model to simulate the injection-production relationship.

The KIGRU architecture, illustrated in Figure 1, employs a dualsubnet design that integrates physical principles with deep learning for reservoir production forecasting. The model comprises two parallel components: the Injection Rate Description Subnet (Net-INJ) and the Volume Change Description Subnet (Net-VOL). Net-INJ processes injection rate time series through a gate function and connection matrix that encodes inter-well spatial relationships, feeding into a GRU network with hidden states (h1, h2) to extract temporal knowledge about injection-production connectivity. Net-VOL jointly processes injection rate and injection pressure data through a similar GRU architecture to characterize volume change dynamics within the reservoir. Both subnets utilize standard GRU cells with reset gates, update gates, and tanh activation functions to maintain temporal memory across time steps. The outputs from Net-INJ and Net-VOL are combined through matrix operations (Hadamard product, matrix multiplication, matrix addition, and matrix subtraction) in the Model Output Part to predict the final Liquid Production Rate for each well.

#### 3.2.1 Injection rate description subnet (Net-INJ)

This subnet is an important component of the knowledge exchange neural network input system, designed to calculate the total water injection rate from each injection well to the production well to be analyzed, and infer inter-well connectivity through a gate function. Assuming the water injection rate and injection pressure data of *M* injection wells are described as Equations 9, 10:

$$WIR = \left[wir_1, \dots, wir_m, \dots, wir_M\right]^T \tag{9}$$

$$P_{INJ} = \begin{bmatrix} p_{inj,1}, & \dots & p_{inj,m}, & \dots & p_{inj,M} \end{bmatrix}^T$$
 (10)

The liquid production rate, bottom hole pressure, and water-cut data of N production wells are represented as Equations 11–13:

$$LPR = \begin{bmatrix} lpr_1, & \dots & lpr_n, & \dots & lpr_N \end{bmatrix}^T$$
 (11)

$$P_{PRO} = \left[ p_{pro,1}, \dots, p_{pro,n}, \dots, p_{pro,N} \right]^{T}$$
 (12)

$$WCT = \left[wct_1, \dots, wct_n, \dots, wct_N\right]^T$$
 (13)

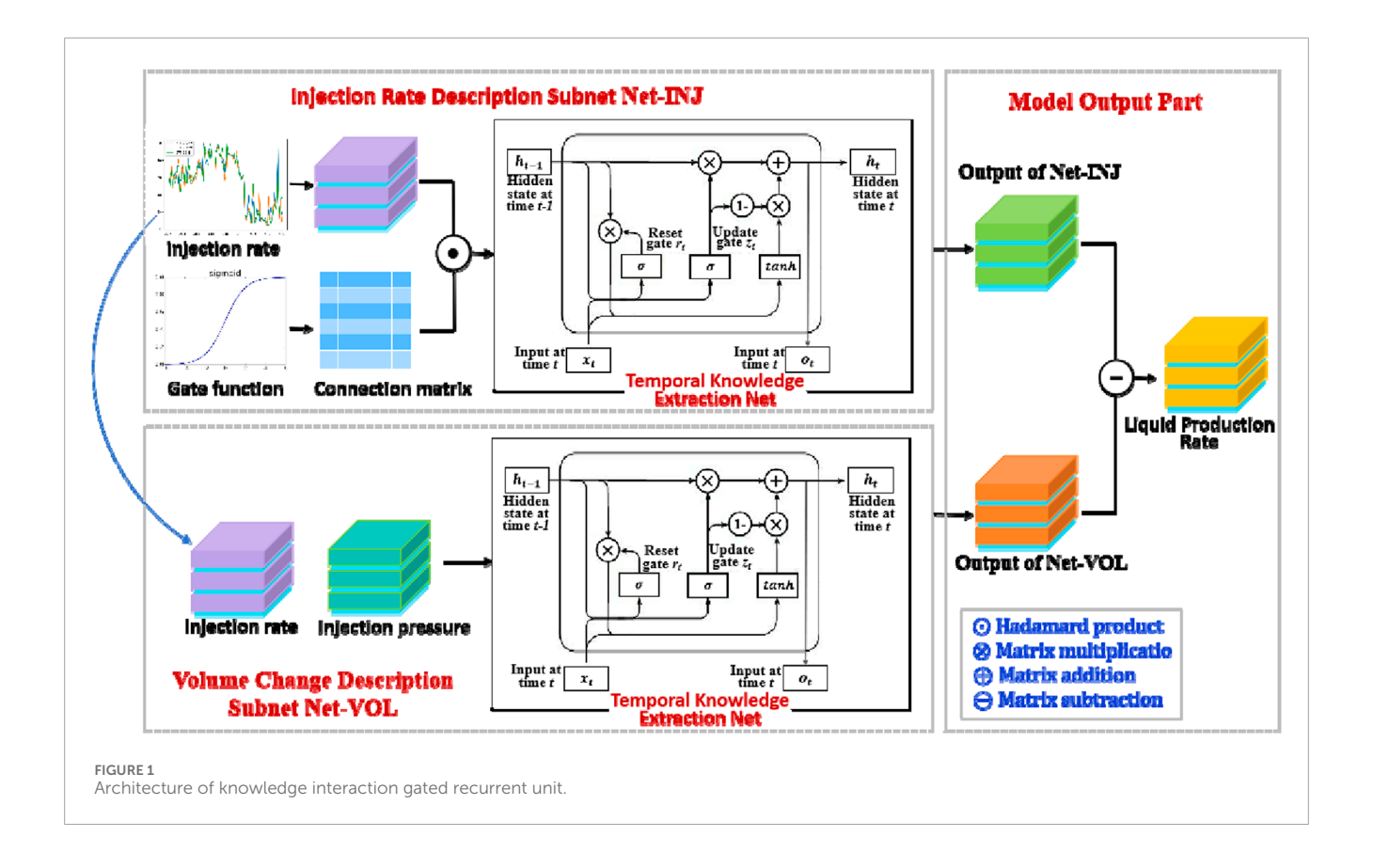
where  $m \in [1,2,...,M]$  and  $n \in [1,2,...,N]$  represent the indices of injection wells and production wells, respectively. Water injection rate WIR, water injection pressure  $P_{INJ}$ , and bottom hole pressure  $P_{PRO}$  are the inputs of the subnet in KIGRU. Meanwhile, the liquid production rate LPR and water-cut WCT of the production well are the output labels of the model.

The input to the injection adjustment module is *WIR*, and the injection-production relationship is measured through the following gate function (Equation 14):

$$gate(\lambda) = \exp(-\lambda^2) \tag{14}$$

It represents the injection-production correspondence between the mth injection well and the nth production well. The mth input of GRU is  $WIR_m \odot gate(WIR_m)$ , i.e.,  $[wir_{m1} \cdot gate(wir_{m1}), wir_{m2} \cdot gate(wir_{m2}), \cdots, wir_{mM} \cdot gate(wir_{mS})]$ , where S denotes the number of samples.

If there is a strong connectivity between the *m*th water injection well and the *n*th production well, the value will approach 1,



indicating that a large amount of water injected from the *m*th water injection well flows into the *n*th production well. Conversely, if the connectivity with the *n*th production well is weak, a lower function value will be assigned in the injection rate description network module, and this value will approach 0.

In KIGRU, the temporal knowledge extraction network utilizes an update gate to determine how much information from past data needs to be passed to the future, while employing a reset gate to decide how much past data to forget. Under this mechanism, the important response signals from past data can be retained, while the redundant or useless signals are eliminated.

The calculation formulas for the update gate and reset gate are as follows (Equations 15, 16):

$$z_t = \sigma(W_z \cdot [h_{t-1}, x_t]) \tag{15}$$

$$r_t = \sigma(W_r \cdot [h_{t-1}, x_t]) \tag{16}$$

where  $\sigma$  is the Sigmoid activation function,  $W_z$  and  $W_r$  are weight matrices, and  $[h_{t-1},x_t]$  is the vector formed by concatenating the hidden state and input at the current time step. Therefore, the calculation process of the candidate hidden state is as follows (Equation 17):

$$\tilde{h}_t = \tanh(W \cdot [r_t \odot h_{t-1}, x_t]) \tag{17}$$

where tanh represents the hyperbolic sine function, W denotes the weight matrix, and  $\odot$  denotes the product of corresponding elements in the matrix, namely, the Hadamard product. The updated formula

for the new hidden state is as follows (Equation 18):

$$h_{t} = (1 - z_{t}) \odot h_{t-1} + z_{t} \odot \tilde{h}_{t}$$
 (18)

The input and output of the temporal knowledge extraction network can be described by Equations 19, 20:

$$SEQ_n = \sum_{m=1}^{M} (gate(x_{mn}) \odot wir_m)$$
 (19)

$$KK_t = Vh_t \tag{20}$$

where  $SEQ_n = [seq_{n1}, seq_{n2}, ..., seq_{nS}]$ ; The input matrix of the temporal knowledge extraction network can be represented as  $SEQ = [SEQ_1, ..., SEQ_n, ..., SEQ_N]^T$ .  $\odot$  is the Hadamard product. V represents the weight matrix of the current output.

The output of the injection rate description subnet can be expressed as Equation 21:

$$INJ_{t} = GRU([SEQ_{t,1}, \dots, SEQ_{t,n}, \dots, SEQ_{t,N}]^{T})$$
(21)

where GRU represents the extraction and calculation of temporal knowledge in Equations 15–19.  $INJ_t$  is the tth column of the total inflow rate matrix INJ for N production wells, calculated after coupling the injection and production data with KIGRU,  $INJECTION \in \mathbb{R}^{N \times S}$ .  $\left[SEQ_{t,1}, \cdots, SEQ_{t,n}, ..., SEQ_{t,N}\right]^T$  represents the total inflow rate of N production wells at time t, which is the tth column of the SEQ matrix.

## 3.2.2 Volume change description subnet (Net-VOL)

The volume change description subnet reflects the fluid change rate within the control volume caused by the compressibility

of underground porous media and fluids. Utilizing the GRU network, the objective is to establish the relationship between the liquid production rate from the production well and the fluid change rate within the control volume. In the volume change description network, not only pressure changes but also water injection rate and liquid production rate are taken into account. In this module, the water injection rate, water injection pressure, and production well pressure data set  $VOL_{INPUT}$  are employed as inputs, which can be denoted as Equation 22:

$$VOL_{INPUT} = \left[WIR, P_{INI}, P_{PRO}\right]^{T} \tag{22}$$

During the simulation of injection-production development dynamics in water-flooding reservoirs, it is necessary to consider the mutual interference between injection and production well groups. Moreover, injection-production dynamic data belong to complex nonlinear time series with time delays. Injected water needs to travel through porous media for several days or even weeks before reaching the bottom of the production well. Therefore, GRU is still used in the volume change description network to capture the dynamic time series behavior hidden in the data, thereby accurately depicting the complex nonlinear relationship between the production rate and the fluid change rate within the control volume. The GRU used is structurally identical to that in the injection rate description network, as shown in Equations 13–17.

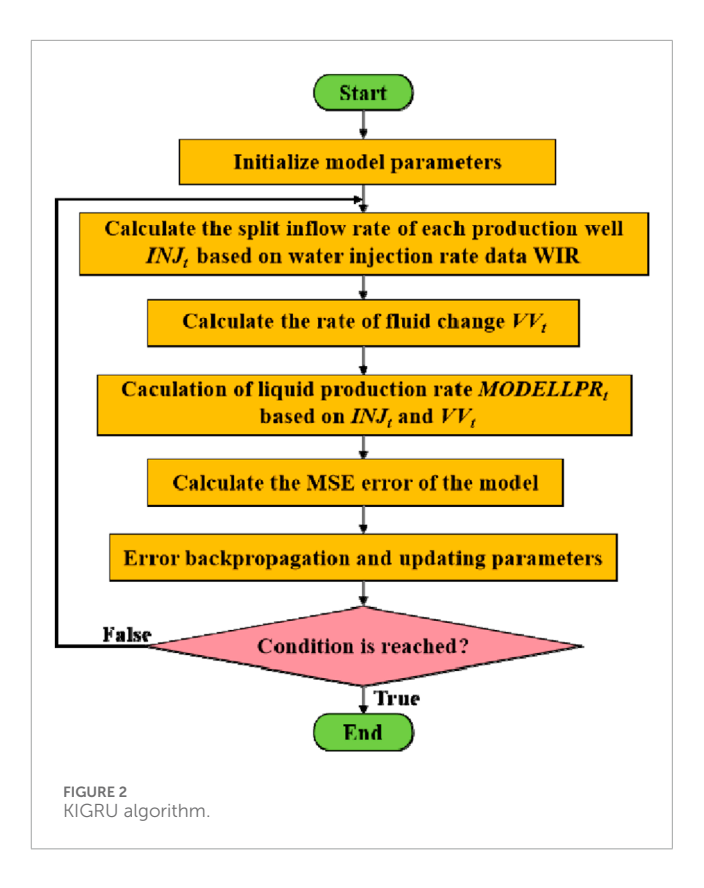
For a given input data set  $VOL_{INPUT}$ , the volume change description subnet can generate the fluid volume change rate  $VV_t$  between the control volumes of each production well through the GRU subnet, which can be denoted as Equation 23:

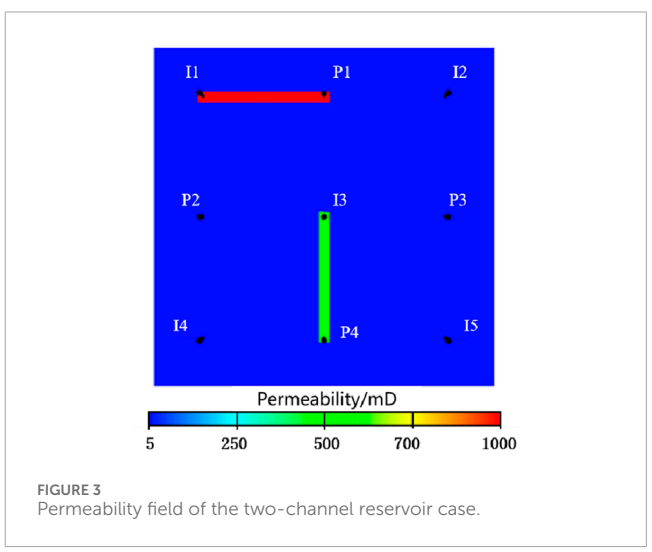
$$VV_t = GRU(VOL_{INPUT})$$
 (23)

where  $VV_t$  represents the tth column of the total liquid production rate matrix VV for N production wells calculated after KIGRU coupled injection and production,  $VV \in \mathbb{R}^{N \times S}$ .

Figure 2 illustrates the training process of reservoir production prediction model. The entire process employs an iterative optimization strategy and consists of the following key steps:

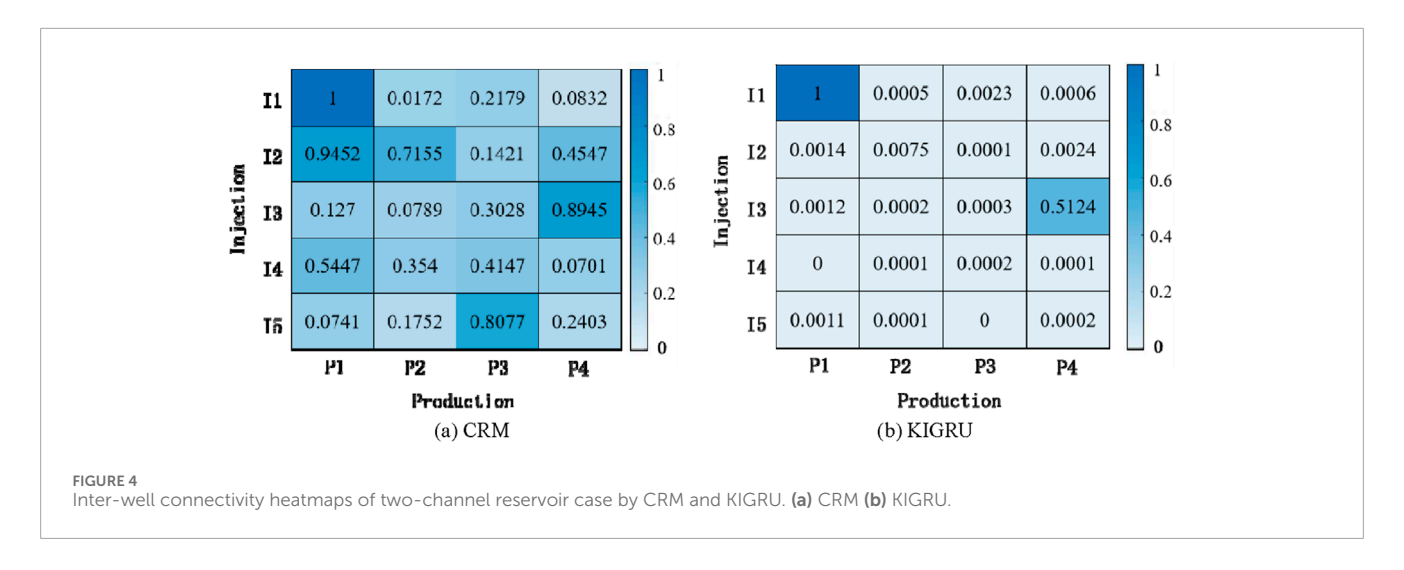
- a. Model Initialization: Initialize model parameters at the beginning
- b. Injection Rate Allocation Calculation: Calculate the split inflow rate for each production well  $(INJ_t)$  based on water injection rate data (WIR)
- c. Fluid Change Rate Calculation: Compute the rate of fluid volume change  $(VV_i)$
- d. Production Prediction: Predict liquid production rate  $(MODELLPR_t)$  based on the calculated  $INJ_t$  and  $VV_t$
- e. Error Calculation: Calculate the Mean Squared Error (*MSE*) between model predictions and actual values
- f. Parameter Update: Update model parameters through error backpropagation mechanism
- g. Convergence Check: Verify if training conditions are met; if not, return to step 2 for continued iteration until convergence, then end training

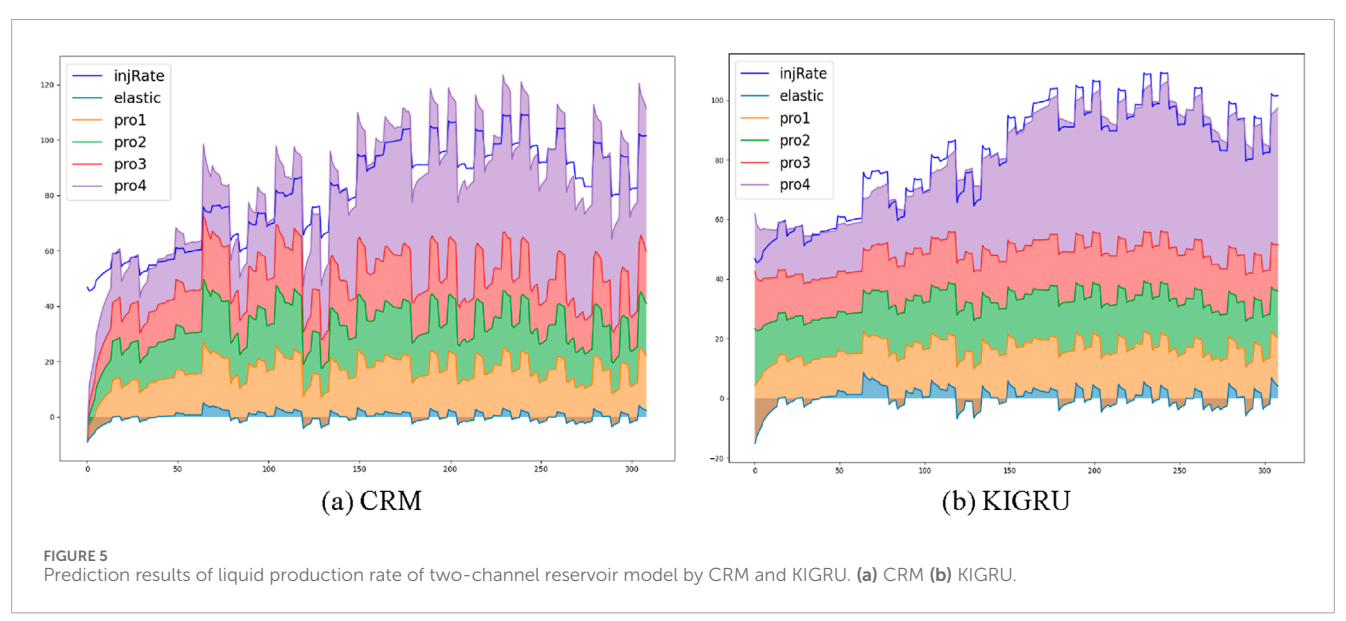




## 3.2.3 Collaborative mechanism of dual subnetworks

The Net-INJ and Net-VOL subnetworks are interconnected through a computational graph, forming a complete injection-production relationship modeling framework. Although the two subnetworks exhibit structural similarity, this is determined by their functional characteristics: Net-INJ specializes in extracting temporal features from injection rate data, while Net-VOL focuses on extracting temporal features from liquid production rate data. Since both injection and production data are essentially flow rate information with similar temporal dynamic characteristics and





physical properties, adopting similar network architectures can better capture the common patterns inherent in such flow rate data.

The collaborative mechanism between the two subnetworks is manifested as follows: the injection feature vectors output by Net-INJ serve as intermediate variables and are jointly input into Net-VOL along with reservoir property parameters. Through this cascaded computational graph approach, an end-to-end mapping from injection signals to production signals is achieved, effectively establishing dynamic connectivity relationships between injection and production wells.

#### 3.2.4 Model output

Based on the material balance equation for water-flooding reservoirs, the simulated liquid production rate of KIGRU can be derived from the injection rate description network and the volume change description network in Equation 24:

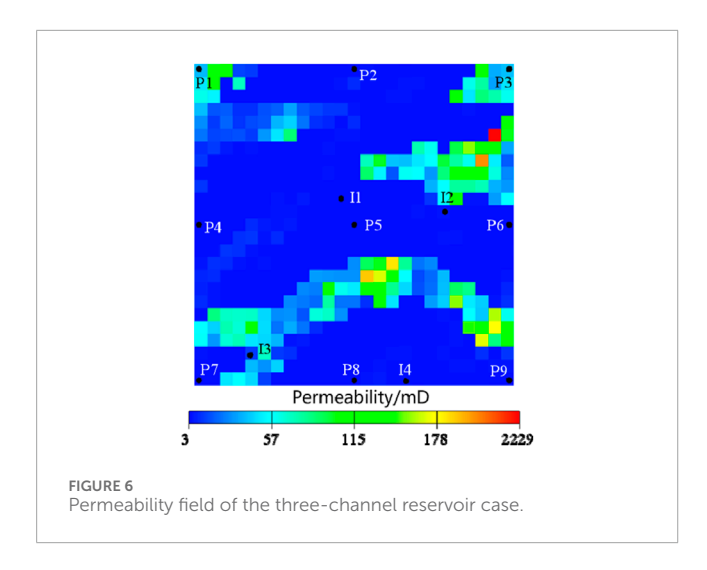
$$MOELLPR_t = INJ_t - VV_t$$
 (24)

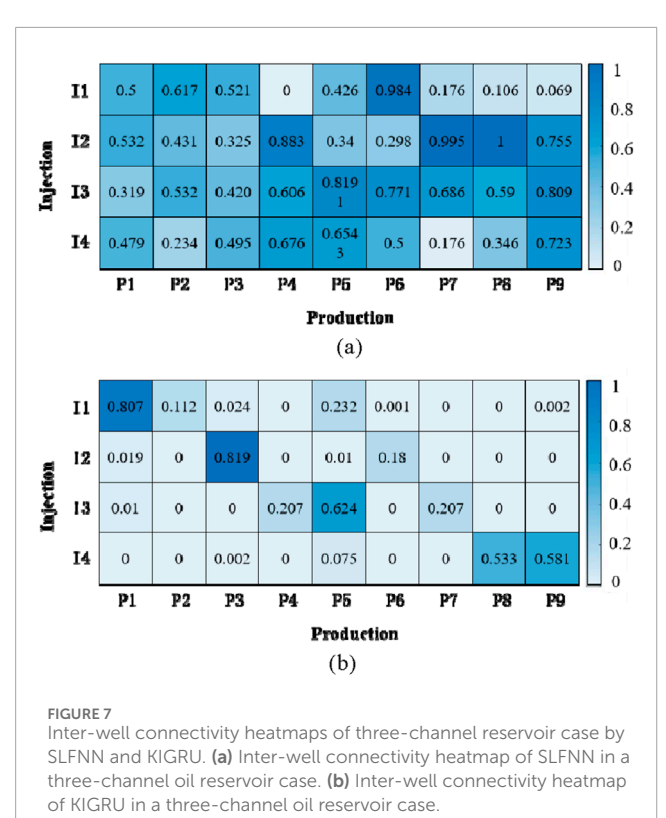
where  $\mathit{INJ}_t$  represents the output of the injection rate description network, corresponding to the water injection rate on the right side of the material balance equation.  $\mathit{VV}_t$  denotes the fluid volume change rate, which corresponds to the left side of the material balance equation. The difference between the two,  $\mathit{MODELLPR}_t$ , corresponds to the liquid production rate on the right side of the material balance equation. When predicting water-cut, the water-cut data  $\mathit{WCT}$  is used to replace  $\mathit{LPR}$  for fitting and predicting water-cut.

The KIGRU model employs mean squared error (MSE) as the loss function and takes into account the influence of the closed boundary constraints of the oil reservoir. Its calculation formula is expressed as follows:

$$LOSS = \frac{1}{S} \sum_{n=1}^{N} \|LPR_n - MODELLPR_n\|^2 + \mu \sum_{m=1}^{M} \left| \left( \sum_{n=1}^{N} gate(wir_{mn}) \right) - 1 \right|$$
(25)

where  $LPR_n$  represents the observed liquid production rate of the nth production well, while  $MODELLPR_n$  denotes the model-output liquid production rate of the nth production well.  $\mu$  is a





coefficient that balances the loss of liquid production rate and the loss due to connectivity constraints. The training process of KIGRU is illustrated in Figure 2.

## 4 Test study on oil reservoir cases

#### 4.1 Two-channel oil reservoir scenario

The two-channel reservoir case, proposed by (Yousef et al., 2006), is a two-dimensional heterogeneous reservoir model composed of a grid with dimensions of  $31 \times 31 \times 1$ , measuring

 $24 \times 24 \times 4$  m. The case includes 5 water injection wells and four production wells, denoted as I1 to I5 and P1 to P4, respectively. The porosity and initial oil saturation of the model are 0.18 and 0.7, respectively. The permeability field of the model is shown in Figure 3, featuring two high-permeability channels, namely, I1-P1 and I3-P4, with permeabilities of 1000mD and 500mD, respectively. The permeability of other areas is uniformly set at 5mD.

This paper compares the inter-well connectivity results of the Capacitance-Resistance Model (CRM) (Yousef et al., 2009) and the proposed KIGRU model on two-channel oil reservoir scenario. The CRM model is a physically-based approach that has been proven to be a powerful tool in reservoir modeling applications. It is capable of analyzing inter-well connectivity with minimal inputs and a small amount of production and water injection history data. The KIGRU model employs a dual-subnet architecture consisting of Net-INJ and Net-VOL to capture injection-production dynamics in oil reservoirs. Net-INJ processes injection rate data through a gate function and connection matrix to model inter-well connectivity, while Net-VOL jointly processes injection rate and pressure to characterize volume changes. Each subnet utilizes two layer GRU networks with 64 hidden units per layer. The model is trained using the Adam optimizer with an initial learning rate of 0.001, a batch size of 32, and sequence lengths of 300 time steps covering meaningful injection-production response cycles. Dropout regularization (0.2) and gradient clipping are applied to prevent overfitting, with training conducted over 100 epochs using early stopping. The outputs from both subnets are fused through matrix operations to predict liquid production rates, enabling the model to learn both data-driven patterns and physics-informed relationships.

Figure 4 illustrates the heatmap of inter-well connectivity analysis between injection and production wells on the two-channel oil reservoir using both CRM and KIGRU methods. The horizontal axis labels represent the production well numbers, denoted as P1~P5, while the vertical axis labels represent the injection well numbers, denoted as I1~ I5. As shown in the figure, both methods have identified the two high-permeability channels, namely, I1-P1 and I3-P4. However, the connectivity of other well pairs in the CRM method exhibits unreasonable results. For instance, the connectivity values obtained for well pairs I2-P1, I2-P2, I2-P4, I4-P1, I4-P2, and I5-P3 in the CRM method are significantly high. Especially for I2-P2, the obtained value of CRM is 0.9452, which is inconsistent with the actual situation. Conversely, KIGRU more accurately portrays the weak connectivity of low-permeability well pairs. Additionally, although the CRM method can distinguish between these two highpermeability channels, its results suggest that I1-P1 and I3-P4 have similar connectivity, which is inconsistent with the actual situation.

Figure 5 illustrates the fluid production prediction results of CRM and KIGRU on the two-channel oil reservoir measured in cubic meters per day (m³/day). From a fitting accuracy perspective, KIGRU demonstrates significant improvements over CRM in characterizing reservoir dynamics. The model achieves superior material balance accuracy, with minimal discrepancy between injection rates (injRate, blue curve) and total fluid production (pro4, purple area), whereas CRM shows notable gaps indicating mass balance errors. KIGRU's more flexible elastic term produces smoother, more physically realistic production profiles for individual wells (pro1-pro4), effectively filtering noise while preserving genuine trends, in contrast to CRM's

TABLE 1 Liquid production rate history matching and prediction performance by SLFNN and KIGRU.

Metric type	Evaluation index	SLFNN	KIGRU
History matching performance	MSE	0.0933 ± 0.0124	0.0113 ± 0.0018
	RMSE	$0.3054 \pm 0.0203$	0.1063 ± 0.0085
	R2	$0.8234 \pm 0.0421$	$0.9812 \pm 0.0034$
Prediction performance	MSE	0.2465 ± 0.0356	0.0189 ± 0.0027
	RMSE	0.4965 ± 0.0359	0.1375 ± 0.0098
	R2	0.8128 ± 0.0567	0.9654 ± 0.0041

The bolded figures are our key focus indicators, reflecting the improvements in our model.

TABLE 2 Comprehensive model performance Comparison.

Noise level	SLFNN prediction MSE	KIGRU prediction MSE
No noise sensitivity (baseline)	0.2465	0.0189
5% Gaussian noise	0.2891	0.0216
10% Gaussian noise	0.3547	0.0267
15% Gaussian noise	0.4623	0.0358

excessive fluctuations suggesting overfitting or inadequate temporal modeling. Additionally, KIGRU demonstrates better peak capture capability around time steps 150–250, maintaining peak magnitudes aligned with injection variations, while CRM exhibits dampened or exaggerated responses. The model also maintains stable temporal consistency in relative producer proportions throughout the time series, reflecting realistic inter-well connectivity, whereas CRM displays erratic changes indicating unstable parameter estimation. Quantitatively, the reduced variance and tighter injection-production coupling in KIGRU predictions translate to lower Mean Squared Error (MSE), validating its superior fitting accuracy and credibility for reservoir production forecasting.

#### 4.2 Three-channel oil reservoir scenario

As shown in the permeability field depicted in Figure 6, the three-channel reservoir scenario (Meng and Karniadakis, 2020) represents a two-dimensional fluvial heterogeneous reservoir model. This model comprises  $25\times25\times1$  grids with dimensions of  $30\times30\times3$  m. The reservoir porosity and initial oil saturation are set at 0.2 and 0.8, respectively. The model incorporates nine production wells and 4 water injection wells.

This paper compares the results of feed-forward neural network model SLFNN and KIGRU model on the three channel reservoir case. Figure 7 shows the heat map of inter-well connectivity between injection and production wells by SLFNN and KIGRU. It can be seen from the figure that SLFNN is difficult to accurately characterize the true connectivity of all injection and production well groups, while KIGRU successfully identifies four high permeability channel well pairs I1-P1, I2-P3, I3-P5 and I3-P4 for the three channel case.

At this time, the mean square error of SLFNN and KIGRU liquid production rate historical fitting and prediction is shown in Table 1 measured in cubic meters per day (m³/day). Quantitative validation using Mean Squared Error (MSE) further confirms KIGRU's superiority. The values are reported in m³/day for both training and testing datasets, where the training set comprises 80% of the historical production data and the remaining 20% serves as the testing set for model validation. The bolded figures are our key focus indicators, reflecting the improvements in our model.

To comprehensively evaluate KIGRU performance, we conducted comparative experiments with traditional SLFNN on liquid production rate prediction. As shown in Table 1, KIGRU achieves MSE of 0.0113 and 0.0189 for history matching and prediction respectively, with  $\rm R^2$  of 0.9812 and 0.9654, significantly outperforming SLFNN (p < 0.001). Robustness tests (Table 2) demonstrate that KIGRU consistently maintains significant performance advantages under 0%–15% noise interference. Notably, KIGRU under high noise still outperforms noise-free SLFNN, confirming exceptional interference resistance. These results demonstrate KIGRU's exceptional accuracy, robustness, and interference resistance.

### 5 Conclusion

In response to the complex underground connectivity of oil reservoirs, this paper constructs a Knowledge Interactive Gated Recurrent Unit (KIGRU) model based on machine learning methods integrated with physical knowledge, aiming to simulate the inter-well flow process in water-flooding reservoirs. KIGRU incorporates reservoir boundary constraints into the model learning criteria to quantitatively describe the split coefficient of water

injection wells, ensuring the reliability of the model in representing inter-well connectivity. The model employs gated recurrent unit modules, leveraging memory and forgetting mechanisms to effectively address the temporal characteristics in water cut prediction, thereby enhancing the model's applicability on the time scale of oil reservoir development. By introducing physical equations of percolation into the machine learning model, the robustness of the model in predicting production indicators and analyzing connectivity issues is effectively improved, making it valuable for practical applications in analyzing inter-well connectivity for injection and production in oil fields. Through numerical simulation experiments of oil reservoirs, the effectiveness of this method in solving production prediction and inter-well connectivity analysis problems is confirmed. The fundamental reason for the model's effectiveness lies in the synergistic effect between physical constraints and GRU architecture: physical constraints ensure that model outputs comply with reservoir flow patterns, while the GRU memory mechanism effectively captures the temporal dependencies of injection-production processes, with physical constraints playing a more critical role in enhancing model reliability. However, model prediction errors primarily stem from two aspects: noise interference in measured data and limitations in the model structure's ability to describe complex reservoir heterogeneity.

Beyond the aforementioned structural deficiencies, several critical limitations must be acknowledged. Regarding computational cost, the dual-subnet GRU architecture with 100-300 training epochs requires significant computational resources, with training time scaling nonlinearly with the number of wells and time steps, potentially limiting real-time optimization applications. In terms of scalability, while effective for moderate-scale problems (4-20 wells), the model's performance and memory requirements for large-scale reservoirs (more than 100 wells) remain untested, as the connection matrix and hidden state dimensions grow quadratically with well count. Concerning reservoir-scale applicability, the current implementation has been validated only on simplified twochannel synthetic scenarios; its transferability to complex fieldscale reservoirs with heterogeneous geology, faults, and irregular well patterns requires substantial investigation. From a data perspective, the model demands continuous, high-quality injection and production data for effective training; sparse or intermittent measurements typical in mature fields may degrade performance. With respect to physical constraint enforcement, while knowledgeinformed, the model lacks hard constraints for thermodynamic consistency and may occasionally violate physical bounds under extrapolation.

Meanwhile, the KIGRU model still requires further research, which will focus on several concrete research directions to enhance the model's practical applicability. First, field data validation: the KIGRU model will be validated using real-world production data from operating oil fields to assess its robustness under actual reservoir conditions with measurement noise and data uncertainties. Second, multiphase flow extension: the current single-phase liquid production framework will be extended to incorporate oil-water-gas three-phase flow dynamics, requiring modifications to both Net-INJ and Net-VOL subnets to handle phase-specific properties and relative permeability effects. Third, well testing integration: coupling KIGRU with transient pressure analysis and well testing data will enable better characterization of near-wellbore

properties and dynamic reservoir parameters. Fourth, natural water influx modeling: incorporating aquifer influx mechanisms into the injection rate description network module will allow the model to adapt to reservoirs with active bottom or edge water drives. Fifth, multi-layer reservoir modeling: developing hierarchical GRU architectures to handle stratified reservoirs with distinct layer properties and inter-layer communication. These targeted improvements will systematically address current limitations and expand the model's applicability to diverse reservoir scenarios.

## Data availability statement

The original contributions presented in the study are included in the article/supplementary material, further inquiries can be directed to the corresponding author.

#### **Author contributions**

YJ: Writing - original draft. LZ: Writing - review and editing.

## Funding

The author(s) declare that no financial support was received for the research and/or publication of this article.

#### Conflict of interest

Author YJ was employed by Exploration and Development Research Institute of Sinopec Shengli Oil Field Company.

The remaining author declares that the research was conducted in the absence of any commercial or financial relationships that could be construed as a potential conflict of interest.

#### Generative AI statement

The author(s) declare that no Generative AI was used in the creation of this manuscript.

Any alternative text (alt text) provided alongside figures in this article has been generated by Frontiers with the support of artificial intelligence and reasonable efforts have been made to ensure accuracy, including review by the authors wherever possible. If you identify any issues, please contact us.

#### Publisher's note

All claims expressed in this article are solely those of the authors and do not necessarily represent those of their affiliated organizations, or those of the publisher, the editors and the reviewers. Any product that may be evaluated in this article, or claim that may be made by its manufacturer, is not guaranteed or endorsed by the publisher.

#### References

Abbasi, J., and Andersen, P. (2024). Application of physics-informed neural networks for estimation of saturation functions from countercurrent spontaneous imbibition tests. SPEJ. 29, 1710–1729. doi:10.2118/218402-pa

Al-Shabandar, R., Jaddoa, A., Liatsis, P., and Hussain, A. J. (2020). A deep gated recurrent neural network for petroleum production forecasting. *Mach. Learn. Appl.* 3, 100013. doi:10.1016/j.mlwa.2020.100013

Alakeely, A., and Horne, R. N. (2020). Simulating the behavior of reservoirs with convolutional and recurrent neural networks. *SPE Reserv. Eval. and Eng.* 23 (03), 0992–1005. doi:10.2118/201193-pa

Almajid, M. M., and Abu-Al-Saud, M. O. (2022). Prediction of porous media fluid flow using physics informed neural networks. *J. Petroleum Sci. Eng.* 208, 109205. doi:10.1016/j.petrol.2021.109205

Chen, G., Li, Y., Zhang, K., Xue, X., Wang, J., Luo, Q., et al. (2021). Efficient hierarchical surrogate-assisted differential evolution for high-dimensional expensive optimization. *Inf. Sci.* 542 (1), 228–246. doi:10.1016/j.ins.2020.06.045

Chung, J., Gulcehre, C., and Cho, K. (2014). Empirical evaluation of gated recurrent neural networks on sequence modeling[J/OL]. Available online at: https://arxiv.org/abs/1412.3555.

Dai, Q.-Y., Zhang, L.-M., Zhang, K., Hao, H., Chen, G.-D., Yan, X., et al. (2025). Integrated optimization of reservoir production and layer configurations using relational and regression machine learning models. *Pet. Sci.* 22 (9), 3745–3759. doi:10.1016/j.petsci.2025.06.001

Fraces, C. G., and Hamdi, T. (2021). "Physics informed deep learning for flow and transport in porous media," in SPE reservoir simulation conference. SPE.

Gu, J., Liu, W., Zhang, K., Zhai, L., Zhang, Y., and Chen, F. (2021). Reservoir production optimization based on surrograte model and differential evolution algorithm. *J. Pet. Sci. Eng.* 205, 108879. doi:10.1016/j.petrol.2021.108879

Haghighat, E., Raissi, M., Moure, A., Gomez, H., and Juanes, R. (2021). A physics-informed deep learning framework for inversion and surrogate modeling in solid mechanics. *Comput. Methods Appl. Mech. Eng.* 379, 113741. doi:10.1016/j.cma.2021.113741

Harp, D. R., O'Malley, D., Yan, B., and Pawar, R. (2021). On the feasibility of using physics-informed machine learning for underground reservoir pressure management. *Expert Syst. Appl.* 178, 115006. doi:10.1016/j.eswa.2021.115006

Hernandez-Mejia, J. L., Pisel, J., Jo, H., and Pyrcz, M. J. (2023). Dynamic time warping for well injection and production history connectivity characterization. *Comput. Geosci.* 7, 159, 178

Huang, Z.-Q., Wang, Z. X., Hu, H. F., Zhang, S. M., Liang, Y. X., Guo, Q., et al. (2024). Dynamic interwell connectivity analysis of multi-layer waterflooding reservoirs based on an improved graph neural network. *Petroleum Sci.* 21 (2), 1062–1080. doi:10.1016/j.petsci.2023.11.008

Jiang, Y., Zhang, H., Zhang, K., Wang, J., Cui, S., Han, J., et al. (2022). Reservoir characterization and productivity forecast based on knowledge interaction neural network. *Mathematics* 10 (9), 1614. doi:10.3390/math10091614

Karpatne, A., Atluri, G., Faghmous, J. H., Steinbach, M., Banerjee, A., Ganguly, A., et al. (2017). Theory-guided data science: a new paradigm for scientific discovery from data. *IEEE Trans. Knowl. data Eng.* 29 (10), 2318–2331. doi:10.1109/tkde.2017.2720168

Li, M., Zhang, J., Tan, X., and Zhang, R. (2024). An interwell connectivity assessment model for polymer flooding short-term development data based on A-LSTM and EFAST methods. *Int. J. Energy Res.* 1 (2024), 6704100. doi:10.1155/2024/6704100

Meng, X., and Karniadakis, G. E. (2020). A composite neural network that learns from multi-fidelity data: application to function approximation and inverse PDE problems. *J. Comput. Phys.* 401 (1), 109020. doi:10.1016/j.jcp.2019.109020

Mudunuru, M. K. (2020). Physics-informed machine learning for real-time unconventional reservoir management. No. LA-UR-19-31611. Los Alamos, NM (United States): Los Alamos National Laboratory LANL.

Nagao, M., Akhil, D.-G., Tsubasa, O., and Sankaran, S. (2024). Physics informed machine learning for reservoir connectivity identification and robust production forecasting. SPE J. 29, 4527–4541. doi:10.2118/219773-pa

Raissi, M., Paris, P., and Karniadakis, G. E. (2019). Physics-informed neural networks: a deep learning framework for solving forward and inverse problems involving nonlinear partial differential equations. *J. Comput. Phys.* 378, 686–707. doi:10.1016/j.jcp.2018.10.045

Tang, M., Liu, Y., and Durlofsky, L. J. (2020). A deep-learning-based surrogate model for data assimilation in dynamic subsurface flow problems. *J. Comput. Phys.* 413, 109456. doi:10.1016/j.jcp.2020.109456

Teng, T., Chen, Y., Wang, Y., and Qiao, X. (2025). *In situ* nuclear magnetic resonance observation of pore fractures and permeability evolution in rock and coal under triaxial compression. *J. Energy Eng.* 151 (4), 04025036. doi:10.1061/jleed9. eyeng-6054

Wang, H., and Chen, S. (2023). Insights into the application of machine learning in reservoir engineering: current developments and future trends. *Energies* 16 (3), 1392. doi:10.3390/en16031392

Wang, N., Chang, H., and Zhang, D. (2021). Theory-guided auto-encoder for surrogate construction and inverse modeling. *Comput. Methods Appl. Mech. Eng.* 385, 114037. doi:10.1016/j.cma.2021.114037

Wang, H., Han, J., Zhang, K., Yao, C., Ma, X., Zhang, L., et al. (2021). An interpretable interflow simulated graph neural network for reservoir connectivity analysis. *SPE J.* 26 (04), 1636–1651. doi:10.2118/205024-pa

Wang, H., Zhang, K., and Liu, C. (2023). "Oilfield intelligent production optimization and system simulation based on ant colony algorithm," in 2023 Asia-Europe Conference on Electronics, Data Processing and Informatics (ACEDPI). IEEE Computer Society.

Wang, L., Zhu, L., Cao, Z., Liu, J., Xue, Y., Wang, P., et al. (2025). Thermomechanical degradation and fracture evolution in low-permeability coal subjected to cyclic heating-cryogenic cooling. *Phys. Fluids* 37 (8), 086617. doi:10.1063/5.0282266

Wen, G., Tang, M., and Benson, S. M. (2021). Towards a predictor for CO2 plume migration using deep neural networks. *Int. J. Greenh. Gas Control* 105, 103223. doi:10.1016/j.ijggc.2020.103223

Xu, J., Zhan, S., Wang, W., Su, Y., and Wang, H. (2022). Molecular dynamics simulations of two-phase flow of n-alkanes with water in quartz nanopores. *Chem. Eng. J.* 430 (1), 132800. doi:10.1016/j.cej.2021.132800

Yousef, A. A., Gentil, P. H., Jensen, J. L., and Lake, L. W. (2006). A capacitance model to infer interwell connectivity from production and injection rate fluctuations. SPE Reserv. Eval. and Eng. 9 (06), 630–646. doi:10.2118/95322-pa

Yousef, A., Jensen, J., and Lake, L. (2009). Integrated interpretation of interwell connectivity using injection and production fluctuations.  $\it Math.~Geosci.~41~(1), 81-102.~doi:10.1007/s11004-008-9189-x$ 

Yu, Z., Sun, Y., Zhang, J., Zhang, Y., and Liu, Z. (2023). Gated recurrent unit neural network (GRU) based on quantile regression (QR) predicts reservoir parameters through well logging data. *Front. Earth Sci.* 11, 1087385. doi:10.3389/feart.2023.1087385

Zeng, X., Zhang, W., Chen, T., Jacobsen, H. A., Zhou, J., and Chen, B. (2022). Evaluating interwell connectivity in waterflooding reservoirs with graph-based cooperation-mission neural networks. *SPE J.* 27 (04), 2443–2452. doi:10.2118/209607-pa

Zhang, H. Q., Jiang, Y. Q., Wang, J., Zhang, K., and Pal, N. R. (2022a). Bilateral sensitivity analysis: a better understanding of a neural network. *Int. J. Mach. Learn. Cybern.* 13 (8), 2135–2152. doi:10.1007/s13042-022-01511-z

Zhang, K., Zuo, Y., Zhao, H., Ma, X., Gu, J., Wang, J., et al. (2022b). Fourier neural operator for solving subsurface oil/water two-phase flow partial differential equation. SPE J. 27, 1815–1830. doi:10.2118/209223-pa